The Role of Charge and Hydrophobicity in Peptide–Lipid Interaction: A Comparative Study Based on Tryptophan Fluorescence Measurements Combined with the Use of Aqueous and Hydrophobic Quenchers†

Anton I. P. M. De Kroon,*,‡ Mark W. Soekarjo,‡ Johannes De Gier,‡ and Ben De Kruijff‡,§

Centre for Biomembranes and Lipid Enzymology and Institute of Molecular Biology and Medical Biotechnology, University of Utrecht, Padualaan 8, 3584 CH Utrecht, The Netherlands

Received February 21, 1990; Revised Manuscript Received May 8, 1990

ABSTRACT: The interaction of interrelated model peptides with model membranes has been studied by techniques based on tryptophan fluorescence. The peptides used are derivatives of the sequence H-Ala-Met-Leu-Trp-Ala-OH, which was designed for this purpose. Several modifications yielded a set of 13 penta- and hexapeptides varying in net charge, hydrophobicity, charge distribution, and the intramolecular position of the tryptophan residue with respect to the charge(s). The affinity of these peptides for small unilamellar vesicles (SUV) consisting of zwitterionic egg phosphatidylcholine (eggPC) and negatively charged beef heart cardiolipin (bhCL) has been investigated in a comparative way. The criteria for affinity comprise (1) intrinsic fluorescence changes upon titration of the peptides with the lipid vesicles, (2) reduced accessibility of the peptides to aqueous quenchers of tryptophan fluorescence (I^- and acrylamide) in the presence of lipid, and (3) exposure to membrane-incorporated fluorescence quenchers, brominated phosphatidylcholines (BrPC). Application of BrPC brominated at different positions along the acyl chains provided information on the membrane topology of the peptides. With respect to the extent of affinity for zwitterionic membranes, the overall hydrophobicity of the peptides is the main determinant. A comparison of the affinity for PC of equally hydrophobic peptides carrying either a single positive or negative charge reveals preferential interaction of the cationic peptide. Both hydrophobic and electrostatic interactions determine the affinity of positively charged mono- and divalent peptides for CL vesicles. The distribution of the charged moieties in divalent positively charged peptides, either both at one end of the molecule or one at each end, has little influence on the affinity of these peptides for CL but does affect the extent of exposure to BrPC. Upon decreasing the surface charge density of the vesicles by diluting CL with increasing amounts of PC, both types of peptides show different behavior. The position of the tryptophan relative to the charged moiety in the peptide molecule is shown to affect the fluorescent properties upon interaction with vesicles. Concerning the membrane topology, all peptides adopt a localization near the membrane surface, with the neutral peptides inserting slightly deeper into the bilayer than the charged peptides. The results allow a comparative analysis of the factors determining the extents and modes of lipid–model peptide interaction; in addition, the validity of the methods applied is discussed.

The functional role that lipid–peptide interactions play in a wide range of biological processes is acquiring growing experimental support. For example, there is increasing evidence in favor of a direct interaction of signal peptides and of mitochondrial presequences with the membrane lipids playing a role at some stage of the membrane insertion or translocation process of precursor proteins [for review see Briggs and Gierasch (1986) and Roise and Schatz (1988)]. Furthermore, lipid–peptide interactions have been implied to catalyze the binding of regulatory peptides to their receptor and to assist in the selection of the proper receptor subtype in the case of interrelated peptides, e.g., the opioid peptides [for review see Sargent et al. (1988)]. Nevertheless, detailed knowledge of the basic molecular mechanisms underlying these interactions is lacking.

The study of model systems consisting of peptides, either chemically synthesized or naturally occurring, interacting with lipid bilayers has proven a valuable contribution to a better understanding of these mechanisms [for review see Jain and Zakim (1987)]. The synthetic peptide approach has the advantage of being flexible: the effects of small changes in the molecule on the lipid–peptide interaction can be determined. Several authors have studied large synthetic α-helix forming peptides which were shown to span the lipid bilayer, as a model for transmembrane proteins (Voges et al., 1987; Davis et al., 1988). Others have investigated much smaller (di-, tri-, tetra-, and penta-) peptides in interaction with model membranes. Jacobs and White (1986, 1987, 1989) have compared, from a thermodynamic point of view, the effect of single amino acid substitutions on the perturbation of DMPC[1] model membranes by tripeptides carrying a single positive charge (Ala-X-Ala-

† This work was supported by the Foundation for Biophysics with financial aid from the Netherlands Foundation for Scientific Research (NWO).

* To whom correspondence should be addressed.

‡ Centre for Biomembranes and Lipid Enzymology.

§ Institute of Molecular Biology and Medical Biotechnology.

[1] Abbreviations: DMPC, dimyristoylphosphatidylcholine; DPPC, dipalmitoylphosphatidylcholine; DOPC, dioleoylphosphatidylcholine; DOPS, dioleoylphosphatidylserine; CL, cardiolipin from beef heart; eggPC, egg yolk phosphatidylcholine; BrPC, brominated phosphatidylcholine(s); 2-Br-PC, 1-palmitoyl-2-(2-bromohexadecanoyl)phosphatidylcholine; 6,7-Br_2-PC, 1-palmitoyl-2-(6,7-dibromostearoyl)phosphatidylcholine; 9,10-Br_2-PC, 1-palmitoyl-2-(9,10-dibromostearoyl)phosphatidylcholine; 11,12-Br_2-PC, 1-palmitoyl-2-(11,12-dibromostearoyl)phosphatidylcholine; 9,10-Br_4-PC, 1,2-bis-(9,10-dibromostearoyl)phosphatidylcholine; t-Boc, *tert*-butyloxycarbonyl; TFA, trifluoroacetic acid; HPLC, high-performance liquid chromatography; SUV, small unilamellar vesicles; naf, normalized accessibility factor.

0006-2960/90/0429-8229$02.50/0

O-*tert*-butyl, with X the variable amino acid).

In the studies mentioned so far peptides were membrane incorporated by hydration of a lipid–peptide mixed film. Spontaneous synthetic peptide–phospholipid vesicle association has been the subject of a number of investigations exploiting the fluorescent properties of an intrinsic tryptophan residue (Dufourcq et al., 1981; Uemura et al., 1983; Jain et al., 1985; Surewicz & Epand, 1984, 1985). These studies demonstrated the importance of overall hydrophobicity and of the absence of charge for the association with PC bilayers and the major role of electrostatics in the interaction of charged di- and tripeptides with anionic phospholipid vesicles.

In order to examine the molecular details of lipid–peptide interaction, especially with respect to membrane insertion and translocation processes, the investigation of a new set of model peptides was commenced. In the present paper the lipid affinity and membrane topology of synthetic peptides based on the sequence H-Ala-Met-Leu-Trp-Ala-OH is addressed. The design of this sequence was guided by the necessity of general hydrophobicity (Ala, Leu, Trp) to ensure a basic level of lipophilicity, and the presence of reporter groups: tryptophan as an intrinsic fluorescent probe and methionine providing a convenient possibility of deuterium labeling for NMR purposes. Several chemical modifications of the amino and carboxyl termini, the introduction of an extra Ile residue, and the replacement of the N-terminal Ala by Arg yielded a series of 13 peptides (Table I), which differ not only in hydrophobicity and net charge but also in the positioning of the charged group(s), particularly with respect to the tryptophan. The tripeptide H-Lys-Trp-Lys-OH was included for reasons of comparison. As for the lipids, the main variable investigated was the membrane surface charge. The peptides' interaction with SUV consisting of beef heart cardiolipin (bhCL) as a model for negatively charged membranes or of egg phosphatidylcholine (eggPC), a zwitterionic phospholipid, has been characterized. Furthermore, the effects of ionic strength and of decreasing the surface charge density by diluting CL with PC on the extent and mode of the interaction with CL vesicles have been addressed.

Lipid–peptide interaction was assayed by steady-state fluorescence measurements of the intrinsic tryptophan. Changes in fluorescence emission intensity and in the wavelength of maximum emission, which occur when the tryptophan enters an environment with a smaller dielectric constant, served as a first indication for membrane interaction. These measurements were supplemented by quenching experiments in which the exposure of the peptides to aqueous and membranous quenchers was determined and from which two additional, sometimes essential, criteria for interaction were derived. As aqueous quenchers the well-established charged I^- (Lehrer, 1971) and the neutral acrylamide (Eftink & Ghiron, 1976) were used. Hydrophobic quenching was accomplished by incorporating brominated phosphatidylcholines (Berlman, 1973) into the vesicles. These act as quenchers of tryptophan fluorescence and, compared to other probes such as nitroxide spin-labeled phospholipids or free fatty acids, either spin-labeled or brominated, are less membrane perturbing (Roseman et al., 1978; East & Lee, 1982; Lytz et al., 1984; Blatt & Sawyer, 1985; McIntosh & Holloway, 1987). Depth-dependent quenching by BrPC with the bromines at different positions along the acyl chains provided some insight into the membrane topology of the peptides. The combined approach of applying intrinsic fluorescence as well as aqueous and hydrophobic quenching measurements to a broad but coherent set of peptides interacting with different lipid systems provided data which allow a detailed comparison of the extents and modes of the interactions. In addition, it revealed some shortcomings of the methods when used separately in the study of peptide–lipid systems.

Experimental Procedures

Materials. The Merrifield resin and all protected amino acids were obtained from Biosearch (San Raphaël, CA), except for N-formylated *N*-t-Boc-tryptophan which was purchased from Peninsula Laboratories (Belmont, CA). The tripeptide H-Lys-Trp-Lys-OH was purchased from Serva (Heidelberg, FRG).

Egg yolk phosphatidylcholine (eggPC) was isolated and purified according to standard procedures. CL from bovine heart was purified according to Smaal et al. (1985). Dioleoylphosphatidylcholine (DOPC) and dipalmitoylphosphatidylcholine (DPPC) were synthesized as described (Van Deenen & De Haas, 1964). The conversion of DOPC to DOPS has been reported earlier (Comfurius & Zwaal, 1977). *cis*-Vaccenic acid (18:1, Δ11) and petroselenic acid (18:1, Δ6) were obtained from Nu-Chek-Prep, Inc. (Elysian, MI), oleic acid (18:1, Δ9) was obtained from Merck (Darmstadt, FRG), and 2-bromohexadecanoic acid was obtained from Janssen Chimica (Beerse, B). 6-Methoxy-*N*-(3-sulfopropyl)quinolinium (SPQ) and *N*-(3-sulfopropyl)-acridinium (SPA) were purchased from Molecular Probes, Inc. (Eugene, OR). All other reagents were analytical grade or better.

Peptide Synthesis, Purification, and Modification. The peptides H-Ala-Met-Leu-Trp-Ala-OH, H-Ala-Ile-Met-Leu-Trp-Ala-OH, and H-Arg-Met-Leu-Trp-Ala-OH were synthesized by solid-phase techniques on Boc-Ala-O-resin using a Biosearch SAM TWO automated peptide synthesizer (peptide synthesis facility Hubrecht Laboratory, Utrecht, E.J.J. Van Zoelen). *N*-Boc-protected amino acids with side-chain-protective groups on the tryptophan (formyl) and the arginine (tosyl) were coupled by standard diisopropylcarbodiimide activation. Peptides were decoupled from the resin by treatment with HF in the presence of anisole as scavenger. In this procedure the arginine-protecting tosyl group was removed. The free peptide was extracted from the resin with 50% acetic acid (v/v) and lyophilized. Deformylation of the peptides' tryptophan was carried out by incubating the peptides at ~1 mM for 24 h at room temperature in 10 mM NH_4HCO_3, pH 9 (Previero et al., 1967), containing a 10-fold molar excess of glycine over peptide to prevent any reattachment of the released formyl groups to the peptide. After lyophilization the peptides were dissolved in 60% (v/v) acetonitrile in water with 0.5% (v/v) TFA and purified by preparative, reverse-phase HPLC on a 25 × 2.2 cm column packed with Si100 (10 μm) Polyol RP-18 (Serva) eluted with linear water–acetonitrile gradients containing 0.1% (v/v) TFA. The resulting peptides with open carboxyl and amino termini were modified in several ways. The negative charge at the carboxyl terminus was removed by methylation using the BF_3/MeOH method (Gattner et al., 1975). The amino terminus was neutralized by reaction with di-*tert*-butyl dicarbonate according to Moroder et al. (1976) using as solvent 2.5% (v/v) H_2O and 2.5% (v/v) triethylamine in ethylene glycol monomethyl ether. Purified t-Boc-protected peptide served as starting point for the coupling of diaminoethane or glycine to the carboxyl terminus. These couplings involved the preparation of the active *N*-hydroxysuccinimide ester of the peptide using dicyclohexylcarbodiimide (DCC) (Anderson et al., 1964). Ethylene glycol monomethyl ether was used as solvent. After removal of dicyclohexylurea by filtration, a molar excess of

Table I: Sequence, Abbreviation, Net Charge, Position of the Tryptophan Residue, and HPLC Characteristics of the Model Peptides Used

peptide	abbreviation[a]	net charge	Trp charge distance[b]	HPLC retention (%)[c]
$^+$N-Ala-Met-Leu-Trp-Ala-O$^-$	AX	0	+4/−2	39.3
$^+$N-Ala-Ile-Met-Leu-Trp-Ala-O$^-$	AIX	0	+5/−2	43.5
$^+$N-Arg$^+$-Met-Leu-Trp-Ala-O$^-$	RX$^+$	+1	+4/−2	40.2
$^+$N-Ala-Met-Leu-Trp-Ala-OMe	AXme$^+$	+1	+4	43.5
$^+$N-Ala-Ile-Met-Leu-Trp-Ala-OMe	AIXme$^+$	+1	+5	47.7
t-Boc-Ala-Met-Leu-Trp-Ala-NH$(CH_2)_2NH_3^+$	bocAXetN$^+$	+1	−3	54.3
$^+$N-Ala-Met-Leu-Trp-Ala-NH$(CH_2)_2NH_3^+$	AXetN^{2+}	+2	+4/−3	37.7
$^+$N-Arg$^+$-Met-Leu-Trp-Ala-OMe	RXme^{2+}	+2	+4	45.0
$^+$N-Lys$^+$-Trp-Lys$^+$-O$^-$	KWK^{2+}	+2	+2/−2	23.2
t-Boc-Ala-Met-Leu-Trp-Ala-O$^-$	bocAX$^-$	−1	−2	53.3
t-Boc-Ala-Ile-Met-Leu-Trp-Ala-O$^-$	bocAIX$^-$	−1	−2	58.5
t-Boc-Ala-Met-Leu-Trp-Ala-Gly-O$^-$	bocAXG$^-$	−1	−3	51.0
t-Boc-Ala-Met-Leu-Trp-Ala-OMe	bocAXme	0		57.0
t-Boc-Ala-Ile-Met-Leu-Trp-Ala-OMe	bocAIXme	0		63.0

[a] The abbreviation X is used for the sequence Met-Leu-Trp-Ala. Other amino acids are indicated by the one-letter symbols; boc indicates the attachment of a *tert*-butyloxycarbonyl group to the amino terminus, me, methylation of the carboxyl group, and etN, the coupling of diaminoethane to the C-terminus. [b] The distance from the tryptophan to the changed moiety is expressed as the number of amino acid residues including the Trp residue itself, separating it from the charge. [c] The percentage acetonitrile in the effluent required to elute the peptide is indicated; for details see Experimental Procedures.

diaminoethane over peptide was added, which was immediately coupled to the peptide. In order to obtain a peptide with positive charges at both termini, the t-Boc group was removed by treatment with TFA. In the case of glycine coupling, the *N*-hydroxysuccinimide ester was purified and lyophilized prior to the addition of excess glycine (in 0.1 M Hepes, pH 8.0) to the peptide dissolved in ethylene glycol monomethyl ether. The yield of these couplings was at least 90% based on the amount of peptide.

The course of all reactions was monitored by analytical reverse-phase HPLC (see below). After removal of the solvent by evaporation the crude products were purified by preparative, reverse-phase HPLC as described above.

The identity of the peptides was confirmed by amino acid analysis on a Kontron Liquimat III after 24 h of hydrolysis with 6 N HCl in vacuo at 110 °C. The final purity of the peptides used was at least 97% as assessed by analytical reverse-phase HPLC on a 25 × 0.45 cm C18 column [Si100 (10 μm) Polyol RP-18, Serva], using the following conditions: solvent system A, 0.1% (v/v) TFA in water; solvent system B, 0.1% (v/v) TFA in 90% (v/v) acetonitrile in water; gradient 10–70% B in 18 min; flow rate 1.5 mL/min; detection at 220 nm. The positions of the elution peaks on the gradient have been listed in Table I.

Concentrations of stock solutions of the peptides in dimethyl sulfoxide (DMSO), 1–5 mM, were quantitated spectrophotometrically by using $\epsilon = 5600\ M^{-1}\ cm^{-1}$ at 280 nm.

Synthesis and Characterization of BrPC. Petroselenic acid, oleic acid, and *cis*-vaccenic acid were reacted with a 2-fold molar excess of Br_2 in chloroform at −20 °C as described (Dawidowicz & Rothman, 1976). After 1 h unreacted Br_2 was removed by washing with a concentrated $Na_2S_2O_3$ solution. The brominated fatty acids were purified by silica gel column chromatography using chloroform–methanol–ammonia (65:35:2 v/v/v) as eluent. DOPC was treated accordingly to yield bis(9,10-dibromostearoyl)-PC (9,10-Br_4-PC).

Coupling of the resulting dibromostearic acids and the commercially available 2-bromohexadecanoic acid to 1-palmitoyllyso-PC, prepared by treatment of DPPC with phospholipase A2 from *Crotalis adamanteus* (Van den Bosch & Van Deenen, 1965), involved conversion to the fatty acid chlorides using $SOCl_2$. After removal of residual $SOCl_2$ by vacuum distillation the crude reaction product was immediately reacted with the lyso-PC (Van Deenen & De Haas, 1964). The BrPC were purified by silica gel column chromatography. The purity was at least 99% as determined by high-performance thin-layer chromatography (HPTLC).

Examination by fast atom bombardment mass spectroscopy (FAB-MS) confirmed the identity of 1-palmitoyl-2-(6,7-dibromostearoyl)phosphatidylcholine (6,7-Br_2-PC), 9,10-Br_2-PC, 11,12-Br_2-PC, and 9,10-Br_4-PC, but revealed the presence of a chlorinated PC component in the 2-Br-PC preparation. Apparently, a Cl–Br substitution occurred during the activation of 2-Br-16:0 to the fatty acid chloride. Application of a sensitive fluorimetric analytical procedure for the determination of halides (Wolfbeis & Urbano, 1983) combined with a phosphorus determination (Rouser, 1975) enabled a reliable quantitation of the halide/phosphorus ratios of the BrPC preparations. The halide ions formed by combustion of the brominated compounds (Schöniger, 1955) were quantitated by their property to quench the fluorescent probes SPQ and SPA according to the Stern–Volmer relationship (see below). The different sensitivities of SPQ and SPA to Cl^- and Br^- quenching allowed the separate determination of the Cl and Br content of the 2-Br-PC preparation. The following results were obtained: the dibromo-PC's (6,7-Br_2-PC, 9,10-Br_2-PC, 11,12-Br_2-PC) were 100% brominated, and the tetrabromo-PC (9,10-Br_4-PC) had a bromine content of at least 96%, whereas the 2-Br-PC preparation contained 37% Br and 63% Cl. An analysis according to the gold chloride method for the determination of free bromide (Tietz, 1970) as modified by Markello et al. (1985) confirmed the value of this Br content in 2-Br-PC. Since chlorinated compounds also have the capability of quenching tryptophan fluorescence (Lakowicz & Hogen, 1980), although less efficiently than brominated ones, a quantitative correction for the decreased Br content cannot be made. However, as a direct comparison of quenching efficiencies of the monobrominated 2-Br-PC and the dibrominated PCs is inherently hampered by the different number of bromines per molecule, the extra decrease in Br content is believed not to interfere seriously with the interpretation of the data, as long as one keeps in mind that the absolute numbers are underestimates of the values that would have been obtained by using 100% brominated 2-Br-PC.

Vesicle Preparation. Throughout all fluorescence experiments SUV were used which were prepared by hydrating a dry lipid film in a buffer containing 100 mM NaCl, 10 mM Tris-HCl, pH 7.5, and 1 mM EDTA (unless otherwise stated), followed by 10 × 30 s of sonication under nitrogen at 50 W with a 0.5-in. flat disrupter tip mounted on a Branson B12

sonifier, while cooling with ice water. The SUV were isolated as the supernatant of a 20-min 37000*g* centrifugation which was applied to remove titanium and any residual multilamellar structures. The phospholipid concentration was determined by phosphorus determination according to Rouser (1975). CL concentrations are always presented on a phosphorus basis.

Fluorescence Measurements. All fluorescence experiments were performed with the buffer mentioned above unless stated otherwise, on an SLM-Aminco SPF-500 C fluorimeter. The solution in the cuvette was continuously stirred and kept at 25 °C. The excitation wavelength was 280 nm (bandwidth 5 nm), and the emission was read at 340 nm (bandwidth 7.5 nm).

(*A*) *SUV Titration Experiments.* The peptide–phospholipid interaction was studied by monitoring the changes in the tryptophan fluorescence spectra of the peptides upon addition of SUV. Small aliquots of a concentrated (~10 mM) SUV suspension were successively added to a solution of 3 μM peptide in the cuvette up to a lipid/peptide ratio (R_i) of 200. At this concentration all peptides are soluble in the buffer. After at least 10 min of equilibration a spectrum was recorded and the emission at 340 nm read. For each amount of lipid added a corrected tryptophan spectrum was obtained by subtraction of the appropriate vesicle blank, after which the wavelength of maximum emission was read. The fluorescence intensity readings were corrected (1) for the vesicle blank (scatter), which at R_i = 200 contributed at most 15% to the total signal, (2) for the dilution caused by the SUV addition, and (3) for the inner-filter effect. The latter correction factor was determined in a parallel lipid titration of the free amino acid tryptophan (Lee, 1982), which was shown not to interact with lipids in aqueous quenching experiments [data not shown; in agreement with London (1986)]. The decrease in fluorescence observed in a tryptophan–lipid titration amounted to 20% of the total signal after scatter correction at R_i = 200. In all lipid titration experiments the absorbance at 280 nm was less than 0.10; the peptides used did not affect the absorbance by the SUV at any R_i, indicating the absence of any peptide-induced vesicle aggregation.

In a number of cases a dissociation constant could be derived from the fluorescence titration curve according to (Surewicz & Epand, 1984; Bashford et al., 1979)

$$\epsilon - 1 = (\epsilon_b - 1) - \frac{K_D(\epsilon - 1)n}{m}$$

where K_D is the dissociation constant of the lipid–peptide complex, m the lipid concentration, and n the number of lipid molecules constituting one peptide binding site; ϵ represents F/F_0, the relative change of fluorescence intensity, and ϵ_b the maximum relative change of fluorescence intensity attainable when all peptide is bound. The parameter $K_D n$, which is obtained as the slope of a plot of $\epsilon - 1$ vs $(\epsilon - 1)/m$, provides a reliable criterion for comparing the lipid affinities of the various peptides; therefore, following Surewicz and Epand (1984), no further attempts were made to resolve K_D and n separately.

(*B*) *Aqueous Quenchers.* Another criterion for lipid–peptide interaction is the change in accessibility of the peptide to aqueous quenchers of tryptophan fluorescence upon introduction of SUV. Iodide (Lehrer, 1971) and acrylamide (Eftink & Ghiron, 1976) were used for this purpose.

KI was added in increasing amounts, from a 4 M stock solution containing 1 mM $Na_2S_2O_3$ to prevent I_2 and I_3^- formation, to the peptide solution at R_i = 0 and R_i = 200, while the fluorescence intensity was read at 340 nm. The values obtained were corrected for dilution and the scatter contribution, derived from a KI titration of a vesicle blank. Data were analyzed according to the Stern–Volmer equation for collisional quenching (Lehrer, 1971): $F_0/F = 1 + K_{SV}[Q]$, where F_0 and F are the fluorescence intensities in the absence and presence of quencher, [Q] is the molar concentration of quencher, and K_{SV} is the Stern–Volmer quenching constant, which equals $k_q\tau_0$, where k_q is the bimolecular rate constant of the collisional quenching process and τ_0 the fluorescence lifetime of the fluorophore in the absence of quencher. The K_{SV} values for the various peptides in the absence of lipid were found to differ depending on net charge and size of the molecule [e.g., for $RXme^{2+}$, K_{SV} = 7.1 M^{-1}; for $AIXme^+$, 6.5 M^{-1}, for AIX, 6.5 M^{-1}, for bocAIX$^-$, 5.5 M^{-1}, and for KWK^{2+}, 9.3 M^{-1}; SD = 0.3 ($N \geq 3$); cf. Lehrer (1971)]. In order to facilitate comparison of the quenching data for the different peptides, a peptide-independent parameter for the accessibility to aqueous quenchers in the presence of lipid is proposed, the normalized accessibility factor (naf), which is defined as $K_{SV}^{R_i=200}/K_{SV}^{R_i=0}$. On the premise that the aqueous quencher does not significantly partition into the membrane bilayer (Eftink & Ghiron, 1976; Chalpin & Kleinfeld, 1983; see also Discussion) the K_{SV} value can be considered a reliable reflection of the bimolecular rate constant for collisional quenching of the peptide present in the aqueous phase, which is determined by the amount of non-vesicle-associated free peptide. As a consequence, it was not necessary to take into account the changes occurring in the fluorescence lifetime when the tryptophan enters a membrane environment [see, e.g., Jain et al. (1985)].

Acrylamide quenching experiments were carried out at an excitation wavelength of 295 nm instead of 280 nm to reduce the absorbance by acrylamide (ϵ^{280} = 4.3 M^{-1} cm^{-1}, ϵ^{295} = 0.24 M^{-1} cm^{-1}). Acrylamide aliquots were added from a 3 M solution to the peptide at R_i = 0 and R_i = 200; fluorescence was monitored at 340 nm. In addition to the type of corrections applied to the KI quenching data, a correction was made for the absorptive screening by acrylamide as described (Parker, 1968). Data were analyzed according to the modified Stern–Volmer equation (Eftink & Ghiron, 1976): $F_0/[F \exp(V[Q])] = 1 + K_{SV}[Q]$, in which the parameter V is introduced to account for the static quenching by acrylamide, which is responsible for the deviation from linearity in Stern–Volmer plots (see, e.g., Figures 2 and 6). Both K_{SV} and V were resolved by approaching $\exp(V[Q])$ by $1 + V[Q]$, which is valid at values smaller than 0.1 M (Eftink & Ghiron, 1981). For the peptides studied K_{SV} values in the range of 12–17 M^{-1} and V values of 1–2.5 M^{-1} were found in agreement with Eftink and Ghiron (1976). In view of the high number of data points required to obtain reproducible values of K_{SV} and V, and because of the inaccuracy introduced when applying acrylamide at R_i = 200 due to the extra scatter corrections needed, it was decided to resort, for practical reasons, to the use of the slope of a linear fit of the Stern–Volmer plot for concentrations up to 60 mM, K_q ($r^2 > 0.98$; see Figure 5b), as criterion for the peptides' accessibility to acrylamide. Due to the heterogeneity in K_q values measured for the different peptides, again the naf (as defined above) was used to facilitate comparison, assuming that V and K_{SV} are similarly affected by a reduced accessibility of the peptide to acrylamide.

(*C*) *Quenching with BrPC.* BrPC were incorporated at various concentrations into PC (10, 25, and 40 molar %) and CL SUV (10, 20, and 30 mol %), and the relative fluorescence change at 340 nm (F/F_0) of the peptides at R_i = 100 was measured for each of the concentrations of the various BrPC. The corrections described for the SUV titration experiments

Table II: Fluorescence Characteristics, Binding Parameters, and Accessibility to Quenchers of Peptides Interacting with EggPC SUV[a]

peptide	$\Delta\lambda_{max}$ (nm), R_i = 200	F/F_0 (340 nm), R_i = 200	K_Dn (mM)	naf[b] (I^-)	naf[b] (acrylamide)	efficiency of quenching by 6,7-Br_2-PC (%)[c]
AIX	0	1.02		0.98	0.97	
AIXme$^+$	1–2	1.18		0.95	0.83	7
bocAXetN$^+$	2	1.22		0.89	0.70	12
RXme^{2+}	0	1.03		0.98	0.98	
bocAX$^-$	1	1.10		0.93	0.77	
bocAXG$^-$	1	1.06		0.96	0.78	6
bocAIX$^-$	1–2	1.22		0.89	0.70	15
bocAXme	3	1.55	0.45	0.70	0.55	21
bocAIXme	4	1.80	0.40	0.65	0.46	40

[a] All data are mean values obtained in at least two independent experiments; the relative error in F/F_0 amounts to 3%, in K_Dn it is 10%; the naf values for I^- and acrylamide contain an absolute error of 0.03, except for bocAXme and bocAIXme, where it amounts to 0.05 in the case of acrylamide quenching. [b] naf denotes the normalized accessibility factor as defined under Experimental Procedures. [c] The quenching efficiency is expressed as $(1 - F/F_0)(100\%)$, where F denotes the fluorescence intensity at 340 nm in the presence and F_0 the fluorescence intensity in the absence of 6,7-Br_2-PC incorporated at 40% (mol/mol) in eggPC SUV, at R_i = 100. The absolute error in the data amounts to 3%.

were applied, and the data of each BrPC were analyzed according to the Stern–Volmer equation for collisional quenching (Berlman, 1973; Markello et al., 1985) by plotting F_0/F vs [BrPC] and determining K_{SV}. In the case of CL SUV the F_0 values originated from measurements of CL SUV containing the appropriate amounts of DOPC. DOPC was chosen for this purpose since its physicochemical properties strongly resemble those of BrPC (East & Lee, 1982).

Binding to Liposomes. The binding of peptides to eggPC liposomes (prepared by hydrating a dry lipid film) was determined by centrifuging a suspension of 5 mM eggPC and 0.1 mM peptide for 30 min at 37000*g* and subsequent quantitation of the peptide remaining in the supernatant by fluorescence measurements as described (De Kroon et al., 1989).

Results

Interaction of Peptides with Uncharged Phospholipid Vesicles. In order to get a first indication of the affinity for uncharged membranes, changes in the fluorescent properties of the peptides' intrinsic tryptophan were monitored upon titration with eggPC SUV. Figure 1 shows that the fluorescence emission intensity of the zwitterionic peptide AIX (the abbreviations for the peptides are explained in Table I) is not affected with increasing amounts of eggPC SUV present; the same results was found for AX (data not shown). The neutral (double-blocked) peptides exhibit an increased fluorescence quantum yield, which is largest for the peptide containing the extra Ile residue (Figure 1a). The net charged peptides (Figure 1b) display an intermediate emission change which is larger for the positively charged peptide, bocAXetN$^+$, than for the negatively charged, bocAXG$^-$. In Table II the relative fluorescence intensity change at a lipid/peptide molar ratio (R_i) of 200 and the accompanying shift in maximum emission wavelength for a more extended set of peptides are summarized. Dissolved in buffer, all peptides exhibit a maximum emission wavelength of 354 nm; with the addition of PC SUV, a small blue shift of the maximum emission wavelength is observed (Table II), the extent of which in most cases parallels the extent of the change in emission intensity. The PC titration curves of the neutral peptides (Figure 1a) allow the quantitative determination of the affinity parameter K_Dn, defined under Experimental Procedures and shown in Table II. The minor intensity changes observed for the other peptides do not allow a reliable K_Dn assessment.

The accessibility of the peptides (in the presence and absence of PC SUV) to the aqueous quenchers, I^- and acrylamide, provides the second criterion for lipid–peptide interaction. From Stern–Volmer plots the normalized accessibility factor

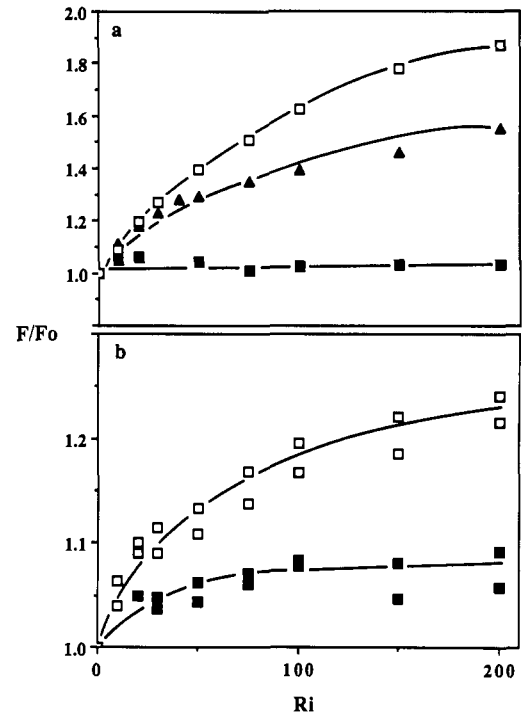

FIGURE 1: Tryptophan fluorescence emission intensities at 340 nm related to the intensity in the absence of lipid (F/F_0) as a function of the molar ratio of eggPC to peptide (R_i) for the following peptides: (panel a) bocAIXme (□), bocAXme (▲), AIX (■); (panel b) bocAXetN$^+$ (□), bocAXG$^-$ (■). The peptide concentration was 3 μM; for experimental details see Experimental Procedures.

(naf) was determined as explained under Experimental Procedures. Comparison of the I^- or acrylamide naf values for the different peptides confirms the order of affinity for eggPC membranes: neutral > single charged > zwitterionic peptides. The naf values obtained with I^- are conspicuously larger than those found with acrylamide (Table II). The divalent positively charged peptides, represented by RXme^{2+} in Table II, hardly show any changes in fluorescence properties upon addition of zwitterionic phospholipid vesicles. The contributions of the hydrophobic residue Ile and the hydrophobic t-Boc group to the interaction with PC SUV are evident, when comparing the peptides carrying a single negative or positive charge.

The decreased exposure to aqueous quenchers upon interaction of the neutral peptides with the PC vesicles is accompanied by an increased accessibility to quenchers present in the hydrophobic phase. Figure 2 shows a Stern–Volmer representation of the fluorescence quenching by 6,7-Br_2-PC incorporated at different concentrations in PC SUV. The linearity of these plots confirms the collisional nature of the

Table III: Fluorescence Characteristics, Binding Parameters, and Accessibility to Aqueous Quenchers of Peptides Interacting with CL SUV[a]

peptide	$\Delta\lambda_{max}$ (nm), R_i = 200	F/F_0 (340 nm), R_i = 200	$K_D n$ (mM)	naf (I^-)	naf (acrylamide)
AIX	0–1	1.05		0.90	0.85
RX^+	0	1.05		0.80	0.75
$AXme^+$	2	1.15	0.35	0.57	0.56
$AIXme^+$	3	1.23	0.22	0.48	0.47
$bocAXetN^+$					
100 mM NaCl	3	1.00		0.38	0.35
0 mM NaCl	3	0.90		0.30[b]	0.23
KWK^{2+}					
100 mM NaCl	1	1.05		–[c]	0.55
0 mM NaCl	4	1.20	0.14	–[c]	0.23
$AXetN^{2+}$	4	1.32	0.07	–[c]	0.44
$RXme^{2+}$	4	1.38	0.08	–[c]	0.35
bocAIXme	3	1.20		0.50	0.52

[a] The absolute error in the naf values of AIX, RX^+, and KWK^{2+} amounts to 0.05; for the errors in the other data, see Table II. [b] K_{SV} value obtained from a linear fit up to 100 mM KI; above this concentration a deviation of linearity occurs in the Stern–Volmer plot. [c] Due to the ionic strength induced peptide release, no K_{SV} could be determined.

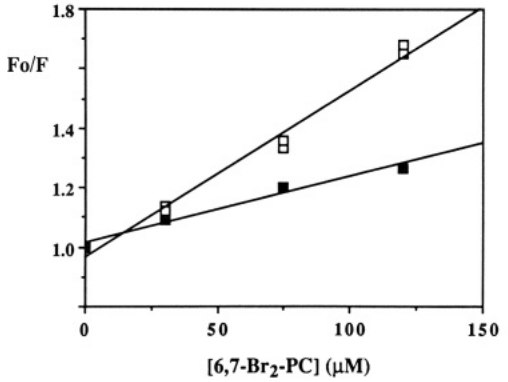

FIGURE 2: Representative Stern–Volmer plot of quenching by BrPC, showing the quenching of bocAIXme (□) and bocAXme (■) by 6,7-Br_2-PC incorporated at 10, 25, and 40% (mol/mol) in eggPC SUV, which corresponds to 30, 75, and 120 μM 6,7-Br_2-PC, at a total lipid concentration of 300 μM; [peptide] = 3 μM.

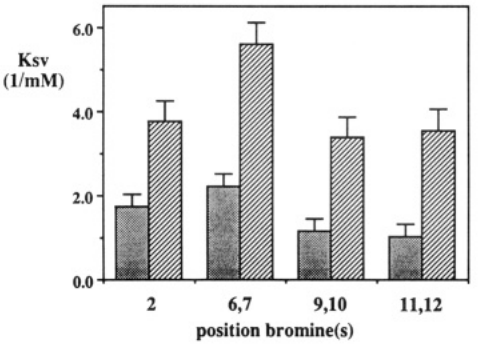

FIGURE 3: Depth-dependent quenching of bocAXme (dotted columns) and bocAIXme (dashed columns) at R_i = 100 by BrPC incorporated in eggPC SUV. The quenching efficiency is expressed as the collisional quenching constant, K_{SV}, and was determined from Stern–Volmer plots. The error bars indicate the average error in the data, obtained in three independent measurements.

quenching process (Berlman, 1973; Markello et al., 1985) and indicates that the incorporation of BrPC hardly affects the membrane affinity of the peptides. The quenching constants obtained from these plots are depicted in Figure 3 for the PCs brominated at different positions. They reveal that the overall quenching of bocAIXme is more efficient than that of the less hydrophobic peptide bocAXme. The efficiency of quenching for both peptides decreases with increasing depth of the bromines (note that the Br content of the monobrominated 2-BrPC is only 37%; see Experimental Procedures). In Table II the efficiencies of quenching by 6,7-Br_2-PC, which reflect the overall efficiency of hydrophobic quenching, have been included for a number of peptides carrying a net charge.

Interaction of Peptides with Negatively Charged Membranes. The neutral peptides represented by boxAIXme in Table III show a fluorescence emission intensity increased upon titration with CL SUV which is relatively small compared to that obtained in a titration with PC (Table II), and which does not allow the determination of a reliable $K_D n$ value. However, the reduction in accessibility to I^- and acrylamide measured for bocAIXme in the presence of CL SUV is similar to that observed for this peptide in the presence of PC SUV.

The negatively charged peptides studied do not show any changes in the tryptophan fluorescence derived interaction criteria upon titration with CL SUV (data not shown). The zwitterionic peptide AIX exhibits small but significant changes in fluorescence intensity and accessibility to I^- and acrylamide (Table III) in the presence of CL SUV. For the zwitterionic peptide lacking the Ile residue, AX, these changes are still smaller (data not shown).

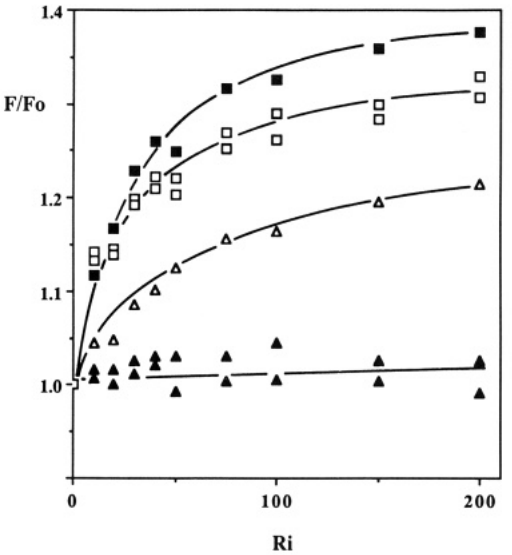

FIGURE 4: Changes in tryptophan fluorescence emission intensity at 340 nm upon titration with CL SUV up to a lipid/peptide ratio of 200 (mol/mol, on a phosphorus basis) of 3 μM of the peptides $RXme^{2+}$ (■), $AXetN^{2+}$ (□), $AIXme^+$ (△), and $bocAXetN^+$ (▲).

Introduction of a net positive charge by replacing the N-terminal Ala by an Arg residue, yielding RX^+, slightly enhances the interaction with CL SUV as judged from the accessibility to aqueous quenchers (Table III). Figure 4 shows the fluorescence emission intensity CL titration curves of $AIXme^+$ and $bocAXetN^+$. Despite the fact that $bocAXetN^+$ does not exhibit a quantum yield increase, its affinity for CL

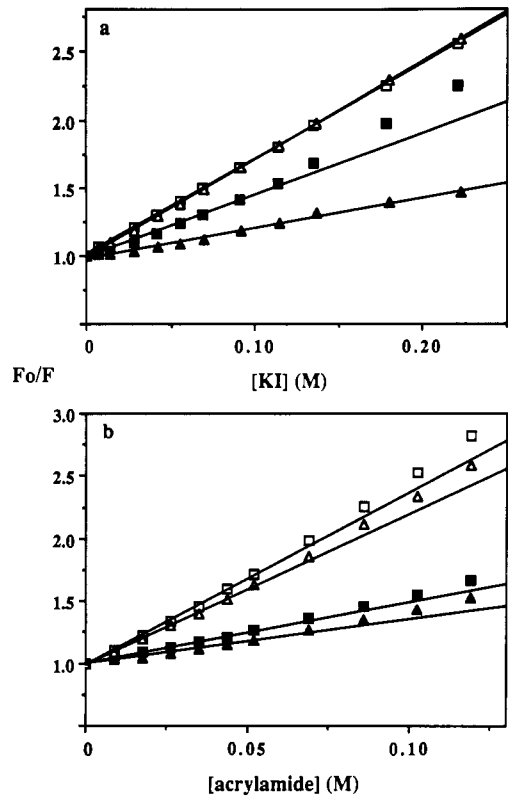

FIGURE 5: Stern–Volmer plots of aqueous quenching by I^- (a) and acrylamide (b) of the peptides $RXme^{2+}$ (squares) and bocAXetN$^+$ (triangles) in the presence (closed symbols) and absence (open symbols) of CL SUV at $R_i = 200$. I^- quenching data of $RXme^{2+}$ were subjected to a linear fit up to 100 mM KI; acrylamide data, up to 60 mM acrylamide.

SUV is larger than that of $AIXme^+$ as evidenced by the normalized accessibility to aqueous quenchers (Table III). Within the class of peptides with a single positive charge the affinity for CL SUV increases with increasing hydrophobicity, going from $AXme^+$ via $AIXme^+$ to boxAXetN$^+$ (Tables I and III). The blue shifts of the wavelengths of maximum emission observed in the experiments with CL are again rather small. For the divalent cationic peptides studied, $RXme^{2+}$ with the charges on one end of the molecule and $AXetN^{2+}$ with a charge at either end, similar fluorescence increases are observed (Figure 4), that of $RXme^{2+}$ being slightly larger, which give rise to calculated K_Dn values of 0.08 and 0.07 mM, respectively (Table III). The affinity of the divalent peptides for CL is evidently larger than that of the monovalent $AIXme^+$ (K_Dn = 0.22 mM). Compared to bocAXetN$^+$, the divalent peptides display a similar affinity for CL as judged from the accessibility to acrylamide (Figure 5b and Table III). I^- quenching of the divalent peptides in the presence of CL SUV reveals a progressive deviation from linearity in the Stern–Volmer plot, illustrated in Figure 5 for $RXme^{2+}$. The membrane association of the divalent peptides may be susceptible to the increased ionic strength resulting from the KI titration.

The influence of ionic strength on peptide binding to CL SUV has been elaborated in Figure 6, which depicts CL titrations, carried out in the absence and presence of NaCl, of KWK^{2+}, a peptide expected to interact mostly in an electrostatic fashion with CL, and bocAXetN$^+$, the most hydrophobic positively charged peptide of the set studied, for which the electrostatic contribution to the binding to CL is likely to be of less importance. At 100 mM NaCl neither peptide exhibits much of a fluorescence intensity change, although the aqueous quenching data indicate a considerable extent of vesicle association, as already noted for bocAXetN$^+$. At 0 mM NaCl

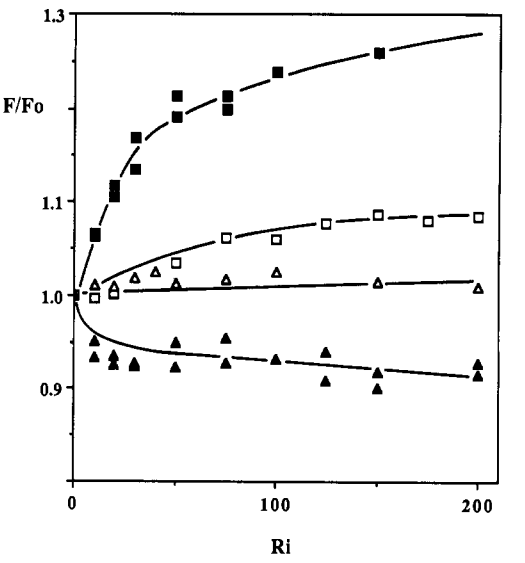

FIGURE 6: Effect of ionic strength on the tryptophan fluorescence intensity changes of KWK^{2+} (squares) and bocAXetN$^+$ (triangles) in the presence of increasing amounts of CL SUV. Buffers used: 100 mM NaCl, 10 mM Tris-HCl, pH 7.5, and 1 mM EDTA (open symbols); 20 mM Tris-HCl, pH 7.5, and 1 mM EDTA (closed symbols).

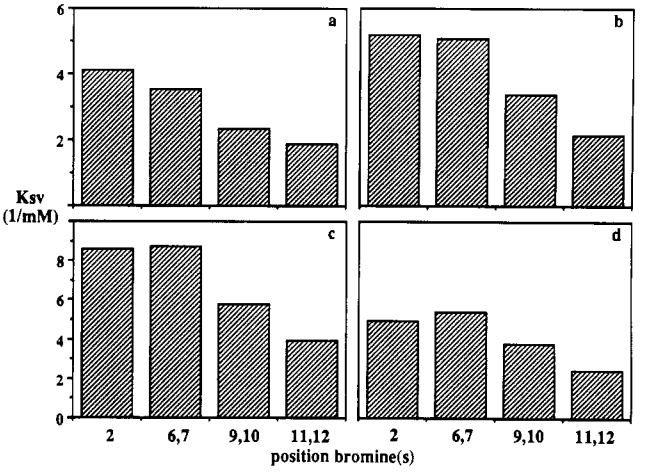

FIGURE 7: Quenching profiles of $AIXme^+$ (a), bocAXetN$^+$ (b), $RXme^{2+}$ (c), and $AXetN^{2+}$ (d) interacting with CL SUV (R_i = 100). Quenching constants, K_{SV}, were determined from the slope of Stern–Volmer plots based on measurements with CL SUV containing 10, 20, and 30% (mol/mol) of the BrPC, as described under Experimental Procedures. The absolute error of K_{SV} in these data amounts to 0.5 mM^{-1}.

the extent of KWK^{2+} binding is enhanced as evidenced by the reduction by a factor of 2 of the degree of exposure to acrylamide (Table III); for bocAXetN$^+$ the extent of the binding increase is less dramatic (Table III). The increased CL affinity is reflected in an enhanced intrinsic fluorescence emission for KWK^{2+} (K_Dn = 0.14 mM) with a concomitant blue shift, whereas a distinct fluorescence decrease is observed for bocAXetN$^+$ when compared to the data at 100 mM NaCl (Figure 6). In the I^- quenching experiments at 0 mM NaCl the effect of increased ionic strength on bocAXetN$^+$ binding to CL is negligible up to 100 mM KI. In contrast, KWK^{2+} is gradually released with the addition of increasing amounts of KI (data not shown).

In Figure 7 the quenching constants (K_{SV}) obtained from linear Stern–Volmer plots of BrPC quenching in the CL system are depicted. The extent of quenching is larger for bocAXetN$^+$ than for $AIXme^+$ in agreement with the higher affinity for CL of the first peptide. A comparison with the

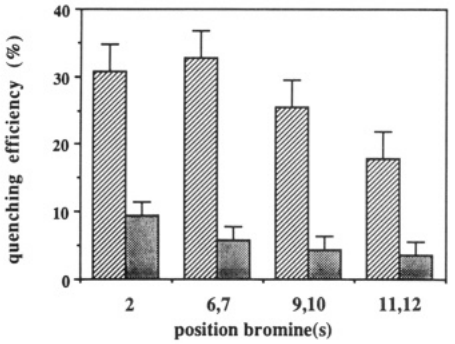

FIGURE 8: Comparison of the depth-dependent quenching efficiencies of $AXetN^{2+}$ (dashed columns) and KWK^{2+} (dotted columns) at 30% (mol/mol) BrPC incorporation in CL SUV, $R_i = 100$. Efficiencies of quenching are expressed as explained in footnote *c* of Table II; the error bars indicate the absolute error.

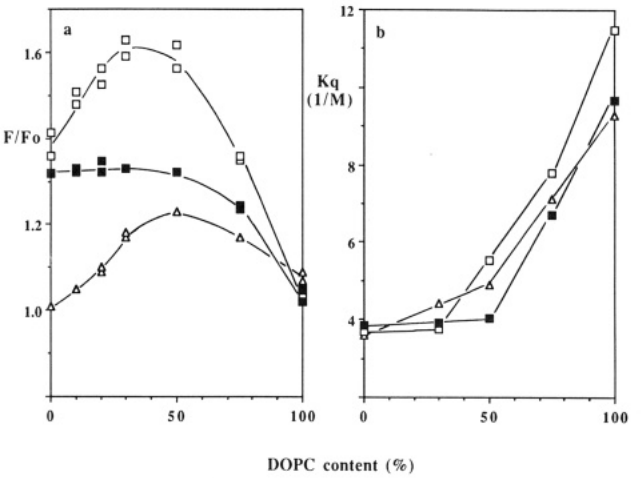

FIGURE 9: Influence of increasing the DOPC content in CL/DOPC SUV on the intrinsic tryptophan fluorescence emission intensity (panel a) and the accessibility to acrylamide (panel b) of the peptides $RXme^{2+}$ (□), $AXetN^{2+}$ (■), and $bocAXetN^{+}$ (△) at $R_i = 100$. In panel *b* each data point represents the quenching constant (K_q) obtained from a single acrylamide titration of the peptide–lipid combination studied.

divalent peptides reveals a similar extent of quenching for $AXetN^{2+}$ whereas the quenching of $RXme^{2+}$ is about twice as efficient. Since $bocAXetN^{+}$, $AXetN^{2+}$, and $RXme^{2+}$ exhibit similar extents of binding to CL SUV (Table III), the differences in exposure to BrPC have to be due to different modes of penetration of the fluorophore. The overall shape of the quenching profiles, however, is the same for these four peptides and indicates a topology of the peptides in the water–membrane interphase with the tryptophan residue inserted into the membrane. In this context a comparison with the quenching profile of KWK^{2+} is useful. Although the extent of KWK^{2+} quenching is relatively small, the shape of the profile clearly shows a stronger bias of the tryptophan residues toward the interphase than that of, e.g., $AXetN^{2+}$ (Figure 8).

The use of CL vesicles containing up to 30 molar % of BrPC or DOPC (for calibration purposes, see Experimental Procedures) raised the question whether a decrease in surface charge density affects the lipid–peptide interaction. Figure 9 shows the effect of increasing the DOPC content in CL SUV on the fluorescence emission intensity and the exposure to acrylamide at a total lipid/peptide ratio of 100 for three positively charged peptides. The data show that below 30% PC the accessibility to acrylamide is virtually independent of the PC content. However, peptides with the charge(s) on one end of the molecule ($RXme^{2+}$ and $bocAXetN^{+}$) display an increase in tryptophan fluorescence emission intensity when the DOPC content is increased, up to ±30% in case of the divalent peptide and even up to ±50% for the more hydrophobic monovalent peptide. In contrast, the fluorescence intensity of $AXetN^{2+}$, which has a charge at both ends of the molecule, remains at the same level under these conditions. Above 50% DOPC incorporation the fluorescence intensities start to decline due to a decrease in the amount of peptide bound as evidenced by the concomitant increased exposure to acrylamide (Figure 9b). The possibility that the increase in intrinsic fluorescence concurring with the constant level of binding at PC contents below 30% respectively 50% originates from changes in the fatty acid composition of the membrane which affect its dielectric constant was excluded in an experiment using DOPS instead of CL, which yielded identical results (not shown).

Discussion

General Considerations. A comparison of the extents and modes of peptide–lipid interaction has been made for a set of related peptides, using four complementary methods based on the fluorescent properties of the peptides' intrinsic tryptophan residue. The variables addressed in this study comprise charge and hydrophobicity of the peptides, charge of the membranes and ionic strength, and additionally the distribution of the charges over the peptide molecule and the intermolecular position of the tryptophan residue with respect to the charged moiety(ies). First, a general survey will be presented which aims at integrating the data and at pointing out the main principles governing model peptide–lipid interaction. Subsequently, several aspects of the study will be discussed in greater detail.

The zwitterionic peptides studied (AX and AIX) show only marginal interaction with lipid bilayers, which is considered to be due to the overall hydrophilic nature of these peptides originating from the two charged moieties, one at each end of the molecule. The larger affinity of AIX for CL than for PC (cf. Tables II and III) probably originates from the lower pH value near the surface of negatively charged bilayers, as compared to that in the bulk aqueous phase (MacDonald et al., 1976). Due to the low surface pH the zwitterionic peptide may bind in the protonated form to CL SUV. The same argument of hydrophilic character explains the lack of interaction of RX^{+} and $AXetN^{2+}$ with PC bilayers (data not shown). In general, for peptides interacting with zwitterionic membranes a certain degree of hydrophobicity was found to be a prerequisite. Within the classes of positively and negatively charged peptides, the order of affinity for PC SUV is in fact reliably predicted by the empirical hydrophobicity scale derived from reverse-phase HPLC retention characteristics (cf. Table I and II). The t-Boc modification was found to contribute more to the hydrophobicity of the peptides than the insertion of an Ile residue and to increase the affinity for PC accordingly (cf. $AIXme^{+}$ and $bocAXetN^{+}$ in Tables I and II). In this context the frequent occurrence of the t-Boc modification in studies concerning lipid–model peptide interaction deserves mentioning (Uemura et al., 1983; Surewicz & Epand, 1984; Jain et al., 1985; Jacobs & White, 1986; Mueller et al., 1986).

The affinity of net charged model peptides for the negatively charged CL membranes is in the first place determined by electrostatic interactions. Peptides carrying a net negative charge, despite their hydrophobicity, do not show any interaction with CL SUV according to the criteria used (data not shown), because of the energy barrier imposed by electrostatic repulsion. With respect to the positively charged peptides, both the value of the net charge and the overall hydrophobicity govern the mode and extent of the interaction with CL SUV,

as will be discussed in more detail below.

The neutral peptides show equal affinity for zwitterionic and acidic model membranes as evidenced by the same extents of reduced accessibility to aqueous quenchers in the presence of PC and CL SUV (Tables II and III), accompanied by similar extents of exposure to membrane-incorporated quenchers of tryptophan fluorescence, the BrPC (data not shown). However, the increase in fluorescence emission intensity is much larger upon interaction with PC than with CL (respectively, $F/F_0 = 1.8$ vs $F/F_0 = 1.2$ at $R_i = 200$ for bocAIXme) and exhibits an almost linear relationship with increasing DOPC contents in CL SUV (data not shown). This difference cannot be attributed to differences in dielectric constant related to the different acyl-chain composition of PC and CL, since similar results were obtained when DOPC and DOPS were used instead of eggPC and CL. It is unlikely that differences in insertion depth are responsible for the divergent intrinsic fluorescence properties, since the profile of quenching by BrPC in the PC system (Figure 3) does not differ from that in the CL system (data not shown). The only explanation remaining is that the negative charge of the lipid head groups affects the attainable fluorescence quantum yield of the tryptophan, either directly by a quenching mechanism or indirectly via an effect on the dielectric constant of the tryptophan's environment, which is situated just below the lipid head groups as judged from the BrPC quenching experiments. Therefore, caution is recommended in comparing peptide–lipid affinity data in different lipid systems, which are based solely on fluorescence intensity measurements. The K_Dn values determined from the titrations of the neutral peptides with PC SUV (Table II) are in good agreement with earlier data on the affinity for DMPC SUV of a neutral pentagastrin derivative (Surewicz & Epand, 1984) and the peptide Boc(LA)$_2$ LWMe (Jain et al., 1985).

I^- versus Acrylamide Quenching. For the forthcoming discussion it is useful to compare the results derived from acrylamide and I^- quenching experiments with each other. Table II and III reveal that in the PC system the accessibility of the peptides in the presence of lipid, represented as the naf, to I^- is larger than to acrylamide, whereas in the CL system the naf values for both aqueous quenchers more or less coincide. The difference observed in the PC system most likely reflects some extent of I^- partitioning into the PC bilayers (Chalpin & Kleinfeld, 1983; Cranney et al., 1983; Lala et al., 1988). In the CL system, I^- is not able to penetrate into the membrane due to electrostatic repulsion. The strong resemblance of the values obtained with I^- and acrylamide in the CL system justifies the use of the naf as defined under Experimental Procedures, including the approaches used to quantitate the acrylamide quenching data.

Positively Charged Peptides Interacting with Negatively Charged Membranes. The extent of interaction of positively charged peptides with CL SUV depends both on electrostatic attraction at the head group level and on hydrophobic interaction between the peptide and the apolar part of the membrane. The affinity for CL was shown to increase with increasing hydrophobicity and by doubling the net charge (Table III).

Interestingly, the binding of bocAXetN$^+$ to CL vesicles is not accompanied by a fluorescence intensity increase as observed for the other positively charged peptides; there is, however, a small blue shift (Table III) and considerable quenching by BrPC (Figure 7b). A decrease in ionic strength, which increases the amount of bocAXetN$^+$ bound according to Gouy–Chapman theory, even gives rise to a reduction of the fluorescence emission quantum yield (Figure 6). The only principal difference between bocAXetN$^+$ and the other peptides carrying a single positive charge is the intramolecular position of the tryptophan with respect to the charged moiety (see Table I). Under the reasonable assumption that the positive charge of the bound peptides resides in the aqueous phase, these observations can be accounted for by a localization of the fluorophore of bound bocAXetN$^+$ in a polar environment in the membrane, i.e., somewhere between the head group and ester bond region where it is still exposed to the bromines along the acyl chains (Figure 7b). In the case of the other peptides, where the distance from tryptophan to charge is larger, the fluorophore enters a more apolar environment, giving rise to the observed fluorescence increase.

From a comparison of the K_Dn values, combined with the normalized accessibility factors for acylamide quenching, it is clear that both divalent peptides, RXme^{2+} and AXetN^{2+}, and the most hydrophobic monovalent peptide studied, bocAXetN$^+$, exhibit the highest affinity for CL SUV, which is similar for the three peptides. However, the mode of interaction of these peptides differs as illustrated, e.g., by the KI quenching experiments. Whereas bocAXetN$^+$ in the presence of CL SUV displays a linear Stern–Volmer plot, the divalent peptides, exemplified by RXme^{2+} in Figure 5a, exhibit a deviation from linearity, which indicates a release of divalent peptide with increasing ionic strength. This reflects the predominance of electrostatic interactions in the binding of the divalent peptides and of hydrophobic interactions in the case of bocAXetN$^+$. The dependence on ionic strength of the association with CL vesicles is strongest for KWK^{2+}, the least hydrophobic peptide studied [see also Dufourcq et al. (1981)].

At first glance, the distribution of the positive charges in the divalent peptides, either on one end of the molecule in RXme^{2+} or on both ends in AXetN^{2+}, hardly affects the interaction with CL SUV. The extent of binding based on K_Dn assessment and accessibility to acrylamide is similar for both peptides; so is the sensitivity to increased ionic strength (data not shown). However, the somewhat larger fluorescence intensity increase observed for RXme^{2+} and the BrPC quenching of RXme^{2+} being twice as efficient as that of AXetN^{2+} (cf. Figure 7c,d) suggest a deeper penetration of the tryptophan of RXme^{2+} as compared to AXetN^{2+}. This difference in attainable penetration depth is explained by the double anchoring of AXetN^{2+} in the head group region vs the single anchoring of RXme^{2+} and the relative positions of the fluorophore with respect to the charges. The difference in membrane surface anchoring is also held responsible for the divergent behavior of the intrinsic fluorescence intensity observed upon decreasing the surface charge of the vesicles by diluting CL with DOPC (Figure 9). Whereas for RXme^{2+} and bocAXetN$^+$ the intrinsic fluorescence intensity increases, that of AXetN^{2+} (and KWK^{2+}, data not shown) remains at a constant level upon increasing the DOPC content under conditions where the amounts of peptide bound does not change. This result probably reflects differences in the depth of insertion of the fluorophore due to the different types of anchoring. In view of the increase in tryptophan fluorescence quantum yield concurring with a constant level of binding, which is observed for the neutral peptides when decreasing the surface charge as discussed above, these data cannot be interpreted in terms of a direction of the changing insertion depth.

The Membrane Topology of the Peptides. The strong dependence of the intrinsic fluorescent properties of a membrane-inserted peptide on the intramolecular position of the tryptophan, apparent from the comparison of bocAXetN$^+$ with

other cationic peptides in the previous section, indicates that the model peptides adopt a defined membrane localization upon binding. The rather small absolute values of the blue shifts of the maximum emission wavelength observed in the systems studied are in agreement with a localization near the membrane surface (Voges et al., 1987). The significantly larger blue shifts found for the comparable pentagastrin derivatives interacting with DMPC may be related to the nature of the acyl chains (Surewicz & Epand, 1984, 1986).

BrPC employed as quenchers of tryptophan fluorescence are suitable for probing the membrane insertion of peptides, since they act over a very short distance and do not drastically perturb the membrane (see the introduction). Other authors have shown, using X-ray diffraction, that the relative positions of the bromines reflect the acyl-chain positions of the bromines (McIntosh & Holloway, 1987). From the fact that linear Stern–Volmer plots were obtained in all BrPC quenching experiments, it can be concluded that incorporation of bromines into the bilayer does not affect the membrane affinity of the peptides. The shapes of the quenching profiles in the CL system (depicted in Figure 7) all look similar and indicate a decreased quenching efficiency with increasing depth of the bromines, in agreement with a localization of the peptides in the lipid–water interphase. The profiles do not allow a subtle distinction in localization between, e.g., the single and double anchored peptides in CL bilayers. Nevertheless, from the overall quenching efficiencies combined with the other affinity parameters, some distinction in the localization of the different peptides could be accomplished as described in the previous section.

Obvious differences in shape of the quenching profiles are observed when comparing KWK^{2+} to the other positively charged peptides interacting with CL (Figure 8). Likewise, a comparison of Figures 3 and 7 reveals that the quenching by 2-Br-PC, compared to that by 6,7-, 9,10- and 11,12-Br_2-PC, of the neutral peptides interacting with PC bilayers is less efficient than that of positively charged peptides interacting with CL bilayers. This suggests that the neutral peptides are capable of inserting somewhat deeper into PC bilayers than the positively charged peptides into CL bilayers than the positively charged peptides into CL bilayers, in agreement with the notion that the charged groups stay in the aqueous phase.

The rather coarse image of the peptides' membrane topology derived from the BrPC quenching experiments is not necessarily inconsistent with the notion that the peptides attain a defined membrane localization. McIntosh and Holloway (1987) have shown that the bromines at the 6,7- and 11,12-positions in BrPC bilayers follow a Gaussian distribution with a $1/e$ half-width of about 4 Å, indicating that the bromines cover rather broad ranges within the bilayer. In addition, the perturbation of the acyl chain order in the bilayer caused by the binding (Jacobs & White, 1987, 1989; De Kroon et al., unpublished results) contributes to the flat shape of the quenching profiles.

At this point it is of interest to compare the quenching efficiencies of 9,10-Br_4-PC and 9,10-Br_2-PC for different peptides. Table IV shows the ratios of the K_{SV} values obtained with these two brominated lipids, in different peptide–lipid systems. These ratios fall in two groups with the larger ones (approximately 1.8) pertaining to the neutral peptides interacting with PC bilayers and the smaller ones (1.3–1.4) characteristic for the positively charged peptides interacting with CL. Since the quenching profiles obtained for neutral peptides in CL and PC bilayers are the same, this difference is not considered due to different acyl chain motions in either

Table IV: Ratios of Quenching Constants (K_{SV}) from Quenching by 9,10-Br_4-PC and 9,10-Br_2-PC in Several Peptide–Lipid Systems[a]

	K_{SV}(9,10-Br_4-PC)/K_{SV}(9,10-Br_2-PC)[b]
bocAXme–PC	1.78
bocAIXme–PC	1.80
$AIXme^+$–CL	1.41
$bocAXetN^+$–CL	1.33
$RXme^{2+}$–CL	1.27
$AXetN^{2+}$–CL	1.31

[a] The lipid/peptide molar ratio is 100 in all systems. [b] The absolute error in the ratios amounts of 0.15.

lipid system. This leaves two possible explanations. The first one takes into account that (1) for tryptophans located closer to the membrane surface the quenching will, to a large extent, be determined by the movements of the acyl chains toward the interphase [cf. Merkle et al. (1987) and Wardlaw et al. (1987)] and (2) the two acyl chains in one phospholipid molecule are not expected to behave stochastically independently of each other in these fluctuations. Consequently, the greater the distance between the tryptophan residue and the bromines, the less the fluorescence of this tryptophan residue will be affected when going from two to four bromines at the 9,10-position. According to this reasoning the charged peptides are less accessible to the bromines, i.e., closer to the membrane surface, than the neutral ones (Table IV), in agreement with the peptides' topology emerging from the quenching profiles as discussed above. The second explanation for the difference in Table IV is that the neutral peptides may have a relatively stronger perturbing effect on the acyl chain order of 9,10-Br_4-PC than the charged ones, which again might be due to a relatively deeper insertion of the neutral peptides.

The conclusion that small tryptophan-containing peptides, including neutral ones, are preferentially localized near the membrane surface has been reached before for other Trp-containing model peptides (Jain et al., 1985; Jacobs & White, 1989). Moreover, the tryptophan residues in cytochrome *b*5 (Tennyson & Holloway, 1986), in apocytochrome *c* (Berkhout et al., 1987), and in a number of membrane-inserting regulatory peptides (De Kroon et al., unpublished results) as well as most of the tryptophans in bacteriorhodopsin (Chatelier et al., 1984) exhibit the strongest fluorescence quenching by probes at the 6,7-position or closer to the surface. This raises the question whether the tryptophan residue itself has an intrinsic preference for an interfacial localization, as suggested earlier by Jacobs and White (1989).

Positive versus Negative Charge in Peptide–PC Interaction. In this section the affinity for eggPC SUV of single charged peptides with respect to the sign of the charge will be examined in detail. A valid comparison of peptides of opposite charge imposes the requirement that the peptides should be equally hydrophobic and sufficiently hydrophobic to enable the measurement of a significant possible difference in the affinity for PC. Since the available negatively charged peptides carry a t-Boc group which enhances the hydrophobicity (Table I), a corresponding positively charged peptide with a t-Boc group, $bocAXetN^+$, was synthesized. Furthermore, the intramolecular position of the tryptophan was taken into account to include the possibility of a comparison based on intrinsic fluorescence changes. For this purpose a glycine residue was attached to $bocAX^-$, yielding $bocAXG^-$, which has a similar tryptophan charge distance as $bocAXetN^+$ (Table I).

From the changes in intrinsic fluorescence (Figure 1b) and from the exposure to aqueous quenchers as well as from the hydrophobic quenching efficiency (Table II), it turns out that $bocAXetN^+$ has a higher PC affinity than $bocAXG^-$ or bo-

cAX$^-$, which behave similarly according to these criteria, despite the different intramolecular tryptophan positions. These negatively charged peptides are slightly less hydrophobic than bocAXetN$^+$ as judged by reverse-phase HPLC (Table I). However, since the insertion of an Ile residue into the negatively charged peptide yielding bocAIX$^-$, rendering it more hydrophobic than bocAXetN$^+$, is required to match the PC binding characteristics of the latter, the conclusion is obvious that positively charged peptides have a higher affinity for PC bilayers than negatively charged ones of equal hydrophobicity. This conclusion was corroborated in an experiment in which the binding of bocAXetN$^+$ and bocAXG$^-$ to eggPC liposomes (multilayered vesicles) was assessed. At concentrations of 0.1 mM peptide and 5 mM PC, 13% of bocAXetN$^+$ vs 3% of bocAXG$^-$ was spun down together with the lipid (for comparison: under these conditions 32.5% of the neutral peptide bocAXme was bound). The preferential binding to PC of the single charged cationic peptides as compared to the anionic ones probably reflects differences in ionization state of the peptides. At pH 7.5 a considerable amount of the terminal amino groups ($pK_a \sim 8$) is deprotonated, rendering the peptides uncharged and consequently more lipophilic. In contrast, the vast majority of the carboxyl groups ($pK_a \sim 3.5$) will be in the charged state at this pH.

In conclusion, the concerted application of intrinsic tryptophan fluorescence measurements, aqueous quenchers, and intrinsic membranous quenchers of tryptophan fluorescence has proven successful in elucidating, in a comparative way, the extents and modes of model peptide membrane binding and insertion. The results obtained, especially those from the cationic peptide–negatively charged membrane system, provide a guideline for the unraveling of the lipid–peptide interactions involved in, e.g., protein translocation and the membrane–receptor binding of regulatory peptides.

ACKNOWLEDGMENTS

We gratefully acknowledge Dr. Jan Van Binsbergen for expert advice on the synthesis and modification of peptides, Mrs. Gerda De Korte-Kool for assistance in the peptide purification, and Mr. Cees Versluis for performing the FAB-MS.

REFERENCES

Anderson, G. W., Zimmerman, J. E., & Callahan, F. M. (1964) *J. Am. Chem. Soc. 86*, 1839–1842.

Bashford, C. L., Chance, B., Smith, J. C., & Yoshida, T. (1979) *Biophys. J. 25*, 63–85.

Berkhout, T. A., Rietveld, A., & De Kruijff, B. (1987) *Biochim. Biophys. Acta 897*, 1–4.

Berlman, I. B. (1973) *J. Phys. Chem. 77*, 562–567.

Blatt, E., & Sawyer, W. H. (1985) *Biochim. Biophys. Acta 822*, 43–62.

Briggs, M. S., & Gierasch, L. M. (1986) *Adv. Protein Chem. 38*, 109–180.

Chalpin, D. B., & Kleinfeld, A. M. (1983) *Biochim. Biophys. Acta 731*, 465–474.

Chatelier, R. C., Rogers, P. J., Ghiggino, K. P., & Sawyer, W. H. (1984) *Biochim. Biophys. Acta 776*, 75–82.

Comfurius, P., & Zwaal, R. F. A. (1977) *Biochim. Biophys. Acta 488*, 36–42.

Cranney, M., Cundall, R. B., Jones, G. R., Richards, J. T., & Thomas, E. W. (1983) *Biochim. Biophys. Acta 735*, 418–425.

Davis, J. H., Clare, D. M., Hodges, R. S., & Bloom, M. (1988) *Biochemistry 27*, 5298–5305.

Dawidowicz, E. A., & Rothman, J. E. (1976) *Biochim. Biophys. Acta 455*, 621–630.

De Kroon, A. I. P. M., De Gier, J., & De Kruijff, B. (1989) *Biochim. Biophys. Acta 981*, 371–373.

Dufourcq, J., Faucon, J. F., Maget-Dana, R., Pileni, M. P., & Hêlène, C. (1981) *Biochim. Biophys. Acta 649*, 67–75.

East, J. M., & Lee, A. G. (1982) *Biochemistry 21*, 4144–4151.

Eftink, M. R., & Ghiron, C. A. (1976) *J. Phys. Chem. 80*, 486–493.

Eftink, M. R., & Ghiron, C. A. (1981) *Anal. Biochem. 114*, 199–227.

Gattner, H. G., Schmitt, E. W., & Naithani, V. K. (1975) *Hoppe-Seyler's Z. Physiol. Chem. 356*, 1465–1467.

Jacobs, R. E., & White, S. H. (1986) *Biochemistry 25*, 2605–2612.

Jacobs, R. E., & White, S. H. (1987) *Biochemistry 26*, 6127–6134.

Jacobs, R. E., & White, S. H. (1989) *Biochemistry 28*, 3421–3437.

Jain, M., & Zakim, D. (1987) *Biochim. Biophys. Acta 906*, 33–68.

Jain, M. K., Rogers, J., Simpson, L., & Gierasch, L. M. (1985) *Biochim. Biophys. Acta 816*, 153–162.

Lakowicz, J. R., & Hogen, D. (1980) *Chem. Phys. Lipids 26*, 1–40.

Lala, A. K., Dixit, R. R., Koppaka, V., & Patel, S. (1988) *Biochemistry 27*, 8981–8989.

Lee, A. G. (1982) *Techniques in Lipid and Membrane Biochemistry II*, B422, Elsevier, Ireland.

Lehrer, S. (1971) *Biochemistry 10*, 3254–3263.

London, E. (1986) *Anal. Biochem. 154*, 57–63.

Lytz, R. K., Reinert, J. C., Church, S. E., & Wickman, H. H. (1984) *Chem. Phys. Lipids 35*, 63–76.

MacDonald, R. C., Simon, S. A., & Baer, E. (1976) *Biochemistry 15*, 885–891.

Markello, T., Zlotnick, A., Everett, J., Tennyson, J., & Holloway, P. W. (1985) *Biochemistry 24*, 2895–2901.

McIntosh, T. J., & Holloway, P. W. (1987) *Biochemistry 26*, 1783–1788.

Merkle, H., Subczynski, W. K., & Kusumi, A. (1987) *Biochim. Biophys. Acta 897*, 238–248.

Moroder, L., Hallett, A., Wünsch, E., Keller, O., & Wersin, G. (1976) *Hoppe-Seyler's Z. Physiol. Chem. 357*, 1651–1653.

Mueller, L., Frey, M. H., Rockwell, A. L., Gierasch, L. M., & Opella, S. J. (1986) *Biochemistry 25*, 557–561.

Parker, C. A. (1968) *Photoluminescence of Solutions*, pp 220–222, Elsevier, New York.

Previero, A., Coletti-Previero, M. A., & Cavadore, J. C. (1967) *Biochim. Biophys. Acta 147*, 453–461.

Roise, D., & Schatz, G. (1988) *J. Biol. Chem. 263*, 4509–4511.

Roseman, M. A., Lentz, B. R., Sears, B., Gibbs, D., & Thompson, T. E. (1978) *Chem. Phys. Lipids 21*, 205–222.

Rouser, G., Fleischer, S., & Yamamoto, A. (1975) *Lipids 5*, 494–496.

Sargent, D. F., Bean, J. W., & Schwyzer, R. (1988) *Biophys. Chem. 31*, 183–193.

Schöniger, W. (1955) *Mikrochim. Acta*, 123–129.

Smaal, E. B., Romijn, D., Geurts van Kessel, W. S. M., De Kruijff, B., & De Gier, J. (1985) *J. Lipid Res. 26*, 633–637.

Surewicz, W. K., & Epand, R. M. (1984) *Biochemistry 23*, 6072–6077.

Surewicz, W. K., & Epand, R. M. (1985) *Biochemistry 24*, 3135–3144.

Surewicz, W. K., & Epand, R. M. (1986) *Biochim. Biophys. Acta 856*, 290–300.

Tennyson, J., & Holloway, P. M. (1986) *J. Biol. Chem. 261*, 14196-14200.
Tietz, N. W. (1977) *Fundamentals of Clinical Chemistry*, pp 1128-1129, W. B. Saunders, Philadephia.
Uemera, A., Kimura, A., & Imanishi, Y. (1983) *Biochim. Biophys. Acta 729*, 28-34.
Van Deenen, L. L. M., & De Haas, G. H. (1964) *Adv. Lipid Res. 2*, 168-229.
Van den Bosch, H., & Van Deenen, L. L. M. (1965) *Biochim. Biophys. Acta 106*, 326-337.
Voges, K. P., Jung, G., & Sawyer, W. H. (1987) *Biochim. Biophys. Acta 896*, 64-76.
Wardlaw, J. R., Sawyer, W. H., & Ghiggino, K. P. (1987) *FEBS Lett. 223*, 20-24.
Wolfbeis, O. S., & Urbano, E. (1983) *Fresenius Z. Anal. Chem. 314*, 577-581.

Kinetics of Disulfide Bond Reduction in α-Lactalbumin by Dithiothreitol and Molecular Basis of Superreactivity of the Cys6-Cys120 Disulfide Bond†

Kunihiro Kuwajima,* Masamichi Ikeguchi,‡ Tatsuro Sugawara, Yoshiki Hiraoka,§ and Shintaro Sugai‡
Department of Polymer Science, Faculty of Science, Hokkaido University, Kita-ku, Sapporo, Hokkaido 060, Japan
Received February 27, 1990; Revised Manuscript Received May 1, 1990

ABSTRACT: Kinetics of disulfide reduction in α-lactalbumin by dithiothreitol are investigated by measuring time-dependent changes in absorption at 310 nm and in CD ellipticity at 270 nm (pH 8.5 or 7.0, and 25 °C). When the disulfide-intact protein is folded, the kinetics are biphasic. The disulfide bond between the half-cystines-6 and -120 is reduced in the fast phase, and the other three disulfide bonds are reduced in the slow phase. The apparent rate constants of the two phases are both proportional to the concentration of dithiothreitol, indicating that both phases are expressed by bimolecular reactions. However, detailed molecular mechanisms that determine the reaction rates are markedly different between the two phases. The slow phase shows a sigmoidal increase in the reaction rate with increasing concentration of a denaturant, urea, and is also accelerated by destabilization of the native state on removal of the bound Ca^{2+} ion in the protein. The disulfide bonds are apparently protected against the reducing agent in the native structure. The fast phase reaction rate is, however, decreased with an increase in the concentration of urea, and the disulfide bond shows extraordinary superreactivity in native conditions. It is 140 times more reactive than normal disulfides in the fully accessible state, and three-disulfide α-lactalbumin produced by the fast phase assumes nativelike structure under a strongly native condition. As ionic strength does not affect the superreactivity of this disulfide bond, electrostatic contributions to the reactivity must be negligible. Inspection of the disulfide bond geometry based on the refined X-ray coordinates of baboon α-lactalbumin [Acharya et al. (1989) *J. Mol. Biol. 208*, 99-127] and comparison of the geometry with those in five other proteins clearly demonstrate that the superreactivity arises from the geometric strain imposed on this disulfide bond by the native structure folding. Relationships of the disulfide strain energy to the protein stability and the disulfide reactivity are discussed.

The disulfide bond is an important factor to stabilize native structures of globular proteins. Experimentally, partial disruption of natural disulfides in a protein often does not radically alter the protein structure, while complete disruption of all the disulfides leads to global unfolding of the protein molecule. The disulfides located on the surface of a protein molecule are often selectively reduced by 2-mercaptoethanol, dithiothreitol (DTT^{SH}_{SH}),[1] or other reducing agents without significant loss of the native structure (DiBella & Liener, 1969; Segawa et al., 1981; Shapira & Arnon, 1969; Sperling et al., 1969; Tamburro et al., 1970; Sondack & Light, 1971; Vincent et al., 1971; Schwarz et al., 1987; Bewley, 1977; Kelley et al., 1987; Pace et al., 1988), but the stability of the folded conformation of the partially disrupted species against thermal or denaturant-induced unfolding is remarkably reduced compared with the disulfide-intact protein. The cleavage of a disulfide cross-link increases the chain entropy of the molecule in the unfolded state, and thereby the stability of the folded state relative to the unfolded one is decreased to such an extent as to be brought about by the entropy increase in the unfolded state (Schellman, 1955; Flory, 1956; Poland & Scheraga, 1965). This aspect of natural disulfides in globular proteins has stimulated recent attempts in protein engineering to enhance protein stability by introducing a new intramolecular disulfide bond (Wells & Powers, 1986; Pantoliano et al., 1987; Villafranca et al., 1987; Matsumura et al., 1989). However, the stability of a protein with a new disulfide bond was not always so enhanced as expected, and, clearly, more studies are required for elucidating the relationship between the disulfide cross-link and the protein stability.

† This work was supported in part by Grants-in-Aid for Scientific Research (General Research 61420050 and 01580258 and Special Project Research 63111001) from the Ministry of Education, Science and Culture of Japan.
* Author to whom correspondence should be addressed.
‡ Present address: Institute of Life Science, Soka University, Tangi-cho, Hachioji, Tokyo 192, Japan.
§ Present address: Department of Microbiology, Keio University School of Medicine, 35 Shinanomachi, Shinjuku-ku, Tokyo 160, Japan.

[1] Abbreviations: 3SS-LA, three-disulfide α-lactalbumin with free cysteinyl residues; CD, circular dichroism; CM-3SS-LA, carboxymethylated three-disulfide α-lactalbumin; DTT^{S}_{S}, oxidized dithiothreitol; DTT^{SH}_{SH}, dithiothreitol; EDTA, ethylenediaminetetraacetic acid; *I*, ionic strength; MOPS, 3-(*N*-morpholino)propanesulfonic acid; TPCK, L-1-(tosylamino)-2-phenylethyl chloromethyl ketone; UV, ultraviolet.

0006-2960/90/0429-8240$02.50/0